

Compositional Analysis of NIST Reference Material Clinker 8486

by

**Paul E. Stutzman
Building and Fire Research Laboratory
National Institute of Standards and Technology
Gaithersburg, MD 20899 USA**

and

**Stefan Leigh
Statistical Engineering Division
National Institute of Standards and Technology
Gaithersburg, MD 20899 USA**

Reprinted from Proceedings from the Twenty-Second International Conference on Cement Microscopy, April 29 - May 4, 2000, Montreal, Quebec, Canada, 22-38 pp., 2000

NOTE: This paper is a contribution of the National Institute of Standards and Technology and is not subject to copyright.

NIST

**National Institute of Standards and Technology
Technology Administration, U.S. Department of Commerce**

From: The Twenty-Second International Conference on Cement Microscopy
April 30 - May 4, 2000
Montreal, Quebec, Canada

Compositional Analysis of NIST Reference Material Clinker 8486¹

Paul E. Stutzman
Inorganic Building Materials Division
National Institute of Standards and Technology

Stefan Leigh
Statistical Engineering Division
National Institute of Standards and Technology

Abstract

Certification of the phase compositions of the three NIST Reference Clinkers will be based upon more than one independent method. The current reference values were established using an optical microscope examination, with additional optical microscope data taken from an ASTM C 1356 round robin. The present X-ray powder diffraction (XRD) study provides the second, independent estimate of the phase abundance. Reitveld refinement of the powder diffraction data allowed calculation of a set of best-fit reference patterns and their scale factors. Because of significant contrast in the linear absorption coefficients of ferrite and periclase, relative to the estimated mean matrix linear absorption coefficient, the scale factors were adjusted for microabsorption effects. The XRD data agree with the optical data with the exception of aluminates. This disagreement may reflect the difficulty in resolving this fine-sized phase using the optical microscope. The XRD data did show greater precision than replicate measurements by microscopy.

Measurements from different sources, laboratories, instruments, and from different methods can exhibit significant between-method variability, as well as distinct within-method variances. The data sets were treated using both unweighted and weighted schemes to establish the best-consensus values and to provide meaningful uncertainties. While the mean values of individual phase abundance do not vary, the 95 % uncertainty level values do. The Mandel-Paule-Vangel-Rukhin method of combining the data sets is favored as this method produces a weighted mean whose weighting scheme does not necessarily skew the consensus value in the direction of the large number of XRD values, and that takes between- as well as within-method variation into account.

¹ Contribution of the National Institute of Standards and Technology. Not subject to copyright in the United States.

Introduction

Improvements in cement production and prediction of cements' performance properties requires the application of material science which, in turn, requires the ability to determine and describe their micro- and macrostructures. Improved methods for determining the phase composition of cements using X-ray powder diffraction will facilitate this understanding. This project, part of the Partnership for High-Performance Concrete Technology at the National Institute of Standards and Technology (NIST), involves the development and testing of analytical methods necessary for characterization of cements. Rietveld refinements to model the complex X-ray powder diffraction (XRD) patterns of cementitious materials will provide phase, chemical, and structural information to more completely characterize them, and so provide an improved basis from which to investigate relationships between cement properties and performance properties.

RM 8486 is one of three NIST reference clinkers used for developing and testing methods of quantitative phase analysis [1]. These clinkers were selected as representative of the range of North American clinker production with respect to phase abundance, crystal size, and crystal distribution. The reference values are currently based upon an optical microscope examination of polished, etched sections. The XRD study is intended to provide both an additional estimate using an independent method of analysis, and data to examine inter- and intra- sample heterogeneity. The combined XRD and optical datasets are intended to establish certified values.

Clinker 8486 is intermediate in crystal size and exhibits heterogeneous phase distribution relative to the other clinkers. Alite occurs as subhedral to anhedral crystals approximately 25 μm in size. Belite occurs in large clusters with an approximate crystal size of 15 μm . Equant periclase crystals up to 15 μm are common throughout the microstructure. A medium- to fine-grained lath-like ferrite, with aluminate filling the inter-lath voids, forms the interstitial constituents.

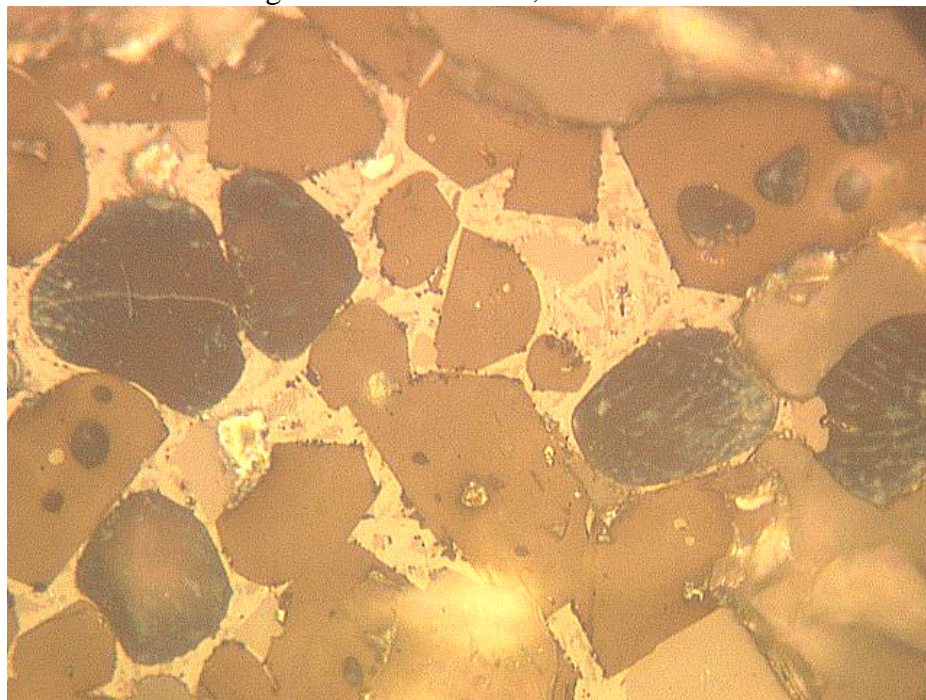


Figure 1. RM 8486 polished section prepared using a 30 s HF vapor etch, field width: 250 μm .

Microscopical Analysis

Clinker petrography has long been used in the examination of clinker materials. ASTM 1356M [2] provides guidance in phase abundance analysis using a microscopical point-count procedure. The advantages of optical microscopy (OM) over chemical analyses are that it provides direct examination of the clinker, characterization of both phase composition and texture, and a rapid, relatively simple method for estimating the phase volume fraction via point count analysis. Procedures for preparation and examination of clinker may be found in Campbell [3].

X-Ray Powder Diffraction

XRD analysis of clinker has been used in cement studies for the past 60 years, and applied in phase abundance analysis over the past 40 years. ASTM 1365 [4] details a standard test method for quantitative phase abundance analysis using XRD (QXRD). X-ray powder diffraction patterns provide phase, chemical, and crystal structure information data that may afford greater understanding of cement property / performance relationships. However, XRD analysis of clinker has proven difficult as the large number of phases results in substantial peak overlap. There is also difficulty in securing suitable pure phase reference standards. This may be addressed using the Rietveld method for X-ray powder diffraction [5]. Public domain code General Structure Analysis System (GSAS) was used to refine the powder diffraction data [6].

The Rietveld method allows standardization of powder diffraction analysis through use of calculated reference diffraction patterns based upon crystal structure models. The result is a set of refined crystal structure models for each phase in the clinker. From these data one can obtain pattern intensity information that may be related to phase abundance. Additional data on the chemical and structural properties of each phase may also be explored relative to selected performance properties. This can be used in research, and for quality-control in cement production, and is now being used to analyze the NIST Reference Clinkers. This method is acceptable under ASTM C1365 where a user is required to qualify their instrument and procedure.

Initial crystal structure models were taken from the literature [7-11]. These models are being incorporated into a cementitious materials crystal structure database currently in development. This database (Figure 2) is a compilation of published structures of cement and related phases, including crystalline phases in mineral admixtures.

Experimental Methods

Sample preparation

A representative sampling of each clinker was obtained through use of a random-stratified sampling scheme and totaled nine samples. Each of these samples was split into replicates designated a and b for a total of 18 specimens. Each replicate was analyzed twice, so for all three clinkers, there were 54 samples and 108 scans. The specimen analysis sequencing was randomized to eliminate any effects of machine drift. For example, RM 8486 sample 1, replicates a and b, were analyzed as runs 12, 46, 32, and 65.

Figure 2. Crystal structure database (in preparation) entry for belite (β -form).

| | | | | | | | | | | |
|--|---|------------------------------------|---------------------------|--------------------------------------|---|-----------------------|------------|------------------------|------------------------------------|------------------------------------|
| Phase: | β -Dicalcium Silicate | Formula: | Ca_2SiO_4 | ICDD: | 33-302 (Iarnite) | | | | | |
| Reference: | K.H. Jost, B. Ziemer and R. Seydel "Redetermination of the Structure of β -Dicalcium Silicate," <i>Acta Cryst.</i> (1977). B33 , 1696-1700 | | | | | | | | | |
| Symmetry: | Monoclinic $P2_1/n$ | Z: | 4 | Mass, Formula Unit: | 3.326 g cm^{-3} | | | | | |
| Cell Parameters (\AA) | | | | | | | | | | |
| a | 5.502 | b | 6.745 | c | 9.297 | | | | | |
| | | b = | 94.59° | | Vol (\AA^3): | | | | | |
| | | | | | 343.9 | | | | | |
| Atomic Parameters | | | | | | | | | | |
| | x | y | z | B (\AA^2) | | | | | | |
| Ca(1) | 0.2738 | 0.3428 | 0.5694 | 0.38 | | | | | | |
| Ca(2) | 0.2798 | 0.9976 | 0.2981 | 0.30 | | | | | | |
| Si | 0.2324 | 0.7841 | 0.5817 | 0.19 | | | | | | |
| O(1) | 0.2864 | 0.0135 | 0.5599 | 0.91 | | | | | | |
| O(2) | 0.0202 | 0.7492 | 0.6919 | 0.67 | | | | | | |
| O(3) | 0.4859 | 0.6682 | 0.6381 | 0.63 | | | | | | |
| O(4) | 0.1558 | 0.6710 | 0.4264 | 0.62 | | | | | | |
| Average interatomic distances | | | | | | | | | | |
| Si - O: 1.63 \AA , Ca - O: 2.88 \AA | | | | | | | | | | |
| Typical bulk belite composition (from Taylor '90, <i>Cement Chemistry</i>) | | | | | | | | | | |
| Na₂O | MgO | Al₂O₃ | SiO₂ | P₂O₅ | SO₃ | K₂O | CaO | TiO₂ | Mn₂O₃ | Fe₂O₃ |
| 0.1 | 0.5 | 2.1 | 31.5 | 0.2 | 0.1 | 0.9 | 63.5 | 0.2 | 0.0 | 0.9 |
| This reference: $(\text{K}_{0.01} \text{Na}_{0.005} \text{Ca}_{0.975} \text{Mg}_{0.01})_2 (\text{Fe}_{0.02} \text{Al}_{0.06} \text{Si}_{0.90} \text{P}_{0.01} \text{S}_{0.01})\text{O}_{3.96}$ | | | | | | | | | | |

The clinkers are provided as millimeter-sized fragments to provide a relatively homogeneous material, yet still be large enough for microscopic analysis. Particle size requirements for XRD necessitate the reduction in particle size to below 10 μm . This maximizes the number of particles analyzed, improves powder homogeneity and packing characteristics, and minimizes microabsorption-related problems.

Each vial of clinker (about 10 g) was split into replicates using the cone-and-quarter technique. The splits were ground individually to fineness (less than about 250 μm) using a mortar and pestle. Final grinding employed a micronizing mill^{2,3} to reduce the clinker to a mean particle size of about 2 μm in 10 min, using 200-proof ethanol (about 5 ml) as a grinding lubricant. The median particle size estimate is based upon a single measurement using an X-Ray absorption particle settling system. The ground clinker was vacuum filtered to remove the ethanol, dried at 60 $^\circ\text{C}$, and then placed in a sealed vial over dessicant in a vacuum dessicator.

² Certain products are identified to more fully describe the analytical procedure. In no case does this imply endorsement by the National Institute of Standards and Technology, nor does it mean that they are the best available for the purpose.

³ McCrone Micronizing mill, McCrone Research, Chicago, Illinois.

Analysis

Data were collected using Cu K α radiation from $2\Theta = 18^\circ$ to 130° , using a step size of 0.02° , a count time of 4 s, and a graphite monochromator. The receiving slit was fixed at 0.2 mm and the variable divergence slit was locked at approximately 0.9° to satisfy the requirement for a constant irradiated volume.

The first step was to establish suitable experiment files to describe the individual phase crystal structures and peak shapes. This was accomplished by refining structure models from the literature (Table 1), compiling them into a structure database, and chemical extractions to concentrate different phase groups. The potassium hydroxide / sucrose extraction (KOSH) concentrates the silicate fraction, the salicylic acid / methanol extraction (SAX) concentrates the interstitial phases, and a 7 % nitric acid in methanol extraction provided a ferrite and periclase residue [12]. This simplified subsequent analyses by allowing refinement of each structure model and the peak shape parameters with less interference from the other constituents. These intermediate models and peak shapes were used for the analyses of the bulk clinker patterns. In essence, the bulk clinker analyses are pattern-fitting exercises using reference standards determined from the extraction residue experiments.

Variables refined for each phase include scale, specimen displacement, background, lattice parameters, atomic coordinates (subject to Si-O or Ca-O bond length constraints), aluminum and iron fractions in ferrite tetrahedral and octahedral sites, peak shapes, and for alite, preferred orientation. Fixing these variables, especially the profile shape parameters, in the subsequent analyses eliminated problematic correlations.

Microabsorption Corrections

Microabsorption results in biased phase fraction estimates where weakly-absorbing phases exhibit greater intensities than expected, while strongly-absorbing phases exhibit lower intensities. Calculation of the linear absorption coefficients for the cement phases (Table 1) and that of a mixture, RM 8486, show that ferrite, periclase, and free lime (when present) may be expected to have the greatest estimate errors unless compensated for. This effect is not problematic in studies utilizing standardization mixtures, as the error was inherent in the standardization curve; however, in Rietveld analyses this effect may be significant.

Fine-grinding reduces microabsorption effects, but trials in our laboratory using binary mixtures of ferrite and periclase show it may still be problematic. Use of the Brindley absorption correction changes the scale factors relative to the differences between the phase and mixture linear absorption coefficients, with an adjustment made for particle size [13].

Table 1. Linear Absorption Coefficients (μ): Cu Ka

| Phase | Composition | m | m / m clinker |
|------------------|---|------------|----------------------|
| Alite | Ca₃SiO₅ | 264 | 0.9 |
| Belite | Ca₂SiO₄ | 294 | 1.0 |
| Aluminate | Ca₃Al₂O₆ | 260 | 0.9 |
| C4AF | Ca₂(Al,Fe)₂O₅ | 496 | 1.7 |
| Free Lime | CaO | 398 | 1.4 |
| Periclase | MgO | 100 | 0.3 |
| Arcanite | K₂SO₄ | 226 | 0.8 |
| RM 8486 | Bulk Clinker | 290 | 1.0 |

Data Presentation and Evaluation

Figure 2 shows a composite plot of the raw data, the calculated peak locations for each phase (tic marks at base of plot), the calculated pattern (green trace), and difference plot. Graphical comparison of the observed versus the calculated pattern, the difference plots, the normalized error distribution and normal probability plots (Figure 3) are perhaps the best means by which to judge the quality of the fit. For the normal probability plot of the residuals, a linear plot with a zero intercept and unit slope indicates that the error is normally distributed. Numerical assessment of the fit is made using the chi-squared value, with lower values reflecting an improvement in the fit. The refinement was stopped when the fit could not be significantly improved.

Quantitative Analysis

Simultaneous refinement of X-ray diffraction patterns of multiple phases allows quantitative analysis using the following relationship, whose variables (aside from Z) are all refined in the fitting process:

$$W_p = (S_p (ZMV)_p) / (S[S (ZMV)])$$

where

- W_p = the mass fraction of phase p,
- S = the Rietveld scale factor,
- Z = the number of formula units per unit cell,
- M = the mass of the formula unit, and
- V = the unit cell volume.

Initial estimates of the phase fractions were used to estimate the linear absorption coefficient of the mixture. A second quantitative estimate using a Brindley absorption correction, based upon a mean particle size of 2 μm , established the final analyses.

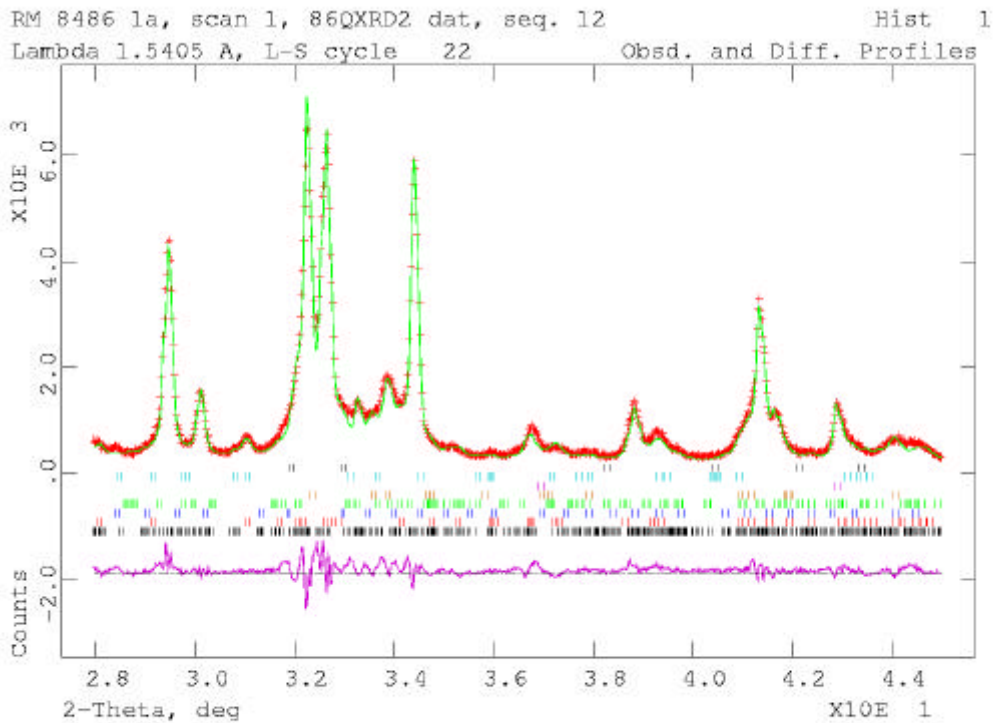
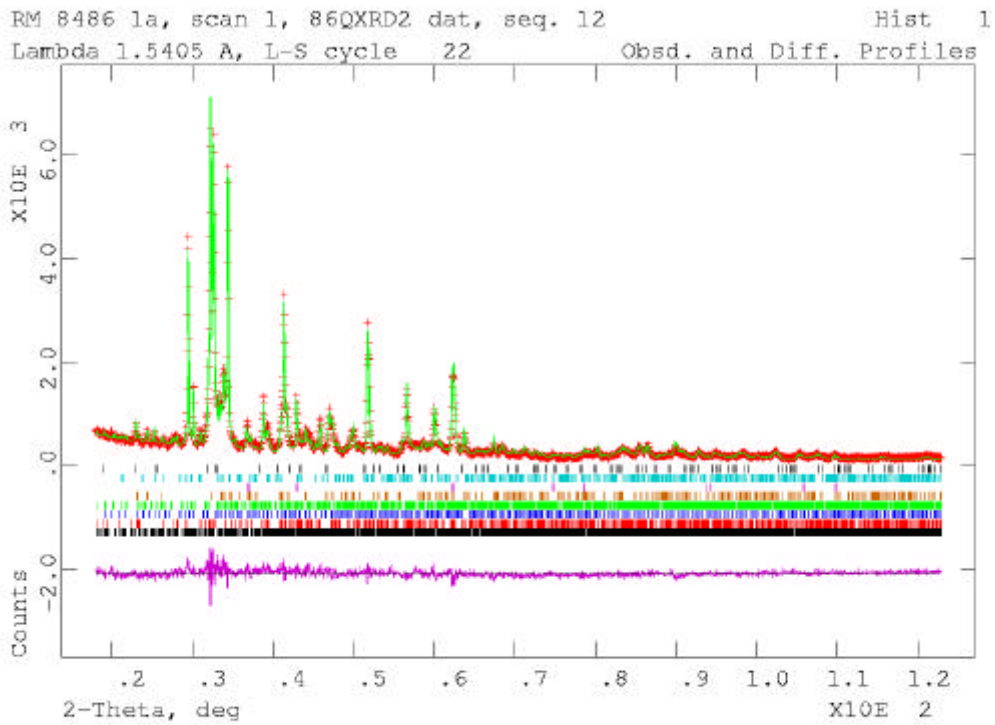


Figure 2. Refined data for sample 1a showing raw, best-fit, and difference curves. The tic marks show peak positions for (bottom up) alite, belite (β and α forms), ferrite, cubic and orthorhombic aluminates, and periclase.

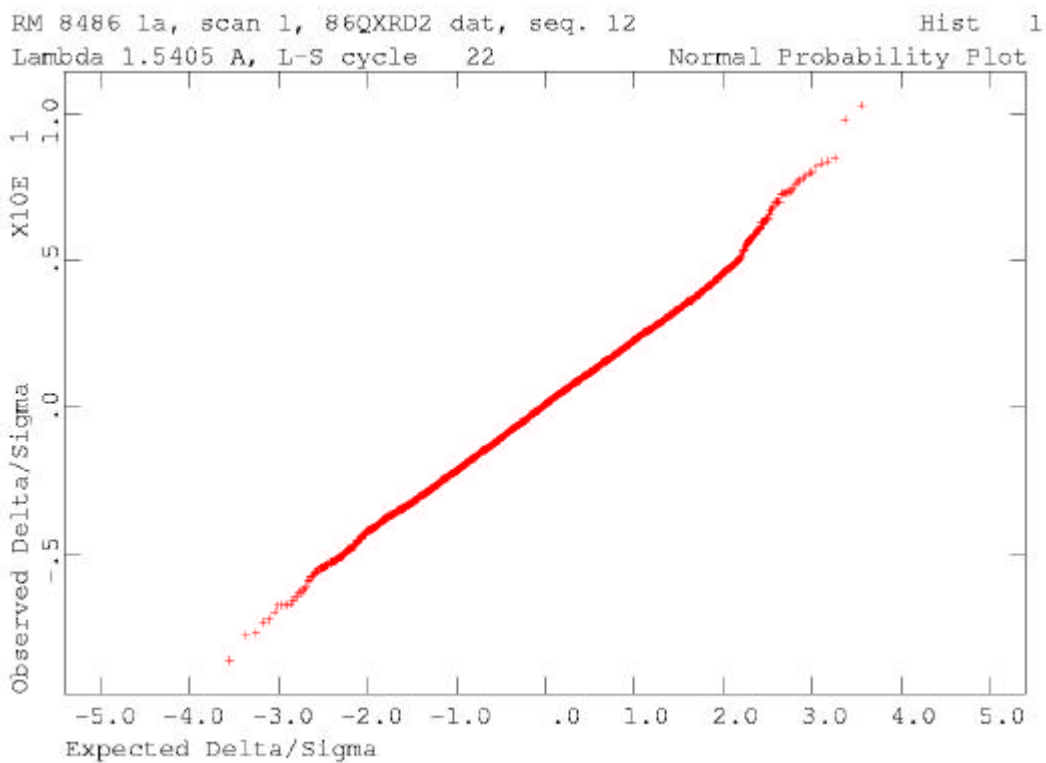
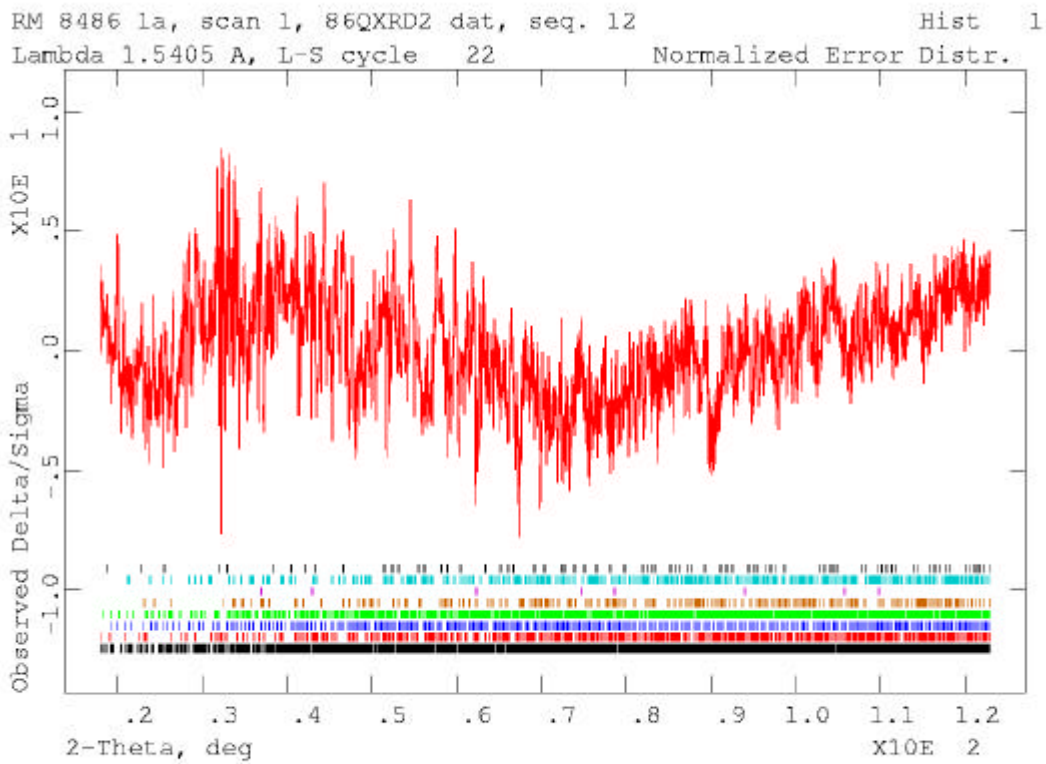


Figure 3. The quality of the fit is reflected through the normalized error distribution. Deviations reflect mis-matches between measured and fit data. A straight normal probability plot of the errors indicates their distribution is well approximated by a Gaussian.

Table 2. Mass fraction (percent) by QXRD, RM 8486 optical data (OM), and round robin data (RR) following ASTM C 1356 [2]. QXRD analysis of nine vials (1-9) with two splits per vial (a, b), with each split analyzed in duplicate (1, 2).

| | Alite | Belite | Ferrite | Aluminate | Periclase |
|-------|-------|--------|---------|-----------|-----------|
| 1a1 | 56.4 | 21.5 | 13.8 | 3.9 | 4.3 |
| 1a2 | 56.8 | 21.8 | 14.0 | 3.3 | 4.0 |
| 1b1 | 55.1 | 21.1 | 16.1 | 3.6 | 4.2 |
| 1b2 | 56.1 | 20.3 | 15.7 | 3.7 | 4.3 |
| 2a1 | 56.8 | 20.9 | 14.6 | 3.5 | 4.2 |
| 2a2 | 56.5 | 21.7 | 14.4 | 3.4 | 4.0 |
| 2b1 | 58.5 | 20.8 | 13.9 | 3.1 | 3.7 |
| 2b2 | 58.5 | 21.0 | 13.5 | 3.2 | 3.8 |
| 3a1 | 56.8 | 21.5 | 14.2 | 3.3 | 4.2 |
| 3a2 | 57.0 | 21.2 | 14.5 | 3.4 | 3.9 |
| 3b1 | 58.6 | 20.4 | 13.7 | 3.3 | 3.9 |
| 3b2 | 57.4 | 20.6 | 14.5 | 3.5 | 4.1 |
| 4a1 | 56.3 | 21.1 | 15.0 | 3.4 | 4.2 |
| 4a2 | 56.2 | 21.5 | 14.9 | 3.3 | 4.1 |
| 4b1 | 56.7 | 20.9 | 14.8 | 3.5 | 4.1 |
| 4b2 | 56.9 | 20.9 | 14.7 | 3.5 | 4.1 |
| 5a1 | 55.8 | 20.6 | 15.7 | 3.5 | 4.4 |
| 5a2 | 55.7 | 20.8 | 15.8 | 3.5 | 4.2 |
| 5b1 | 57.2 | 21.1 | 14.1 | 3.4 | 4.2 |
| 5b2 | 57.1 | 21.0 | 14.1 | 3.4 | 4.3 |
| 6a1 | 56.9 | 21.5 | 14.1 | 3.4 | 4.0 |
| 6a2 | 56.8 | 21.4 | 14.1 | 3.4 | 4.3 |
| 6b1 | 57.3 | 20.7 | 14.2 | 3.6 | 4.2 |
| 6b2 | 57.0 | 20.5 | 15.0 | 3.5 | 3.9 |
| 7a1 | 55.9 | 21.4 | 14.9 | 3.5 | 4.3 |
| 7a2 | 56.5 | 20.7 | 14.8 | 3.5 | 4.6 |
| 7b1 | 56.5 | 21.5 | 14.3 | 3.4 | 4.3 |
| 7b2 | 56.9 | 21.1 | 14.2 | 3.6 | 4.1 |
| 8a1 | 56.7 | 21.2 | 14.4 | 3.5 | 4.2 |
| 8a2 | 57.0 | 21.1 | 14.3 | 3.5 | 4.0 |
| 8b1 | 56.9 | 20.6 | 15.0 | 3.4 | 4.1 |
| 8b2 | 56.3 | 21.1 | 14.8 | 3.5 | 4.2 |
| 9a1 | 55.8 | 21.4 | 15.1 | 3.5 | 4.3 |
| 9a2 | 56.9 | 20.8 | 14.6 | 3.5 | 4.2 |
| 9b1 | 56.1 | 21.0 | 15.3 | 3.5 | 4.1 |
| 9b2 | 57.2 | 20.8 | 14.8 | 3.4 | 3.8 |
| OM1 a | 59.0 | 23.0 | 13.0 | 1.1 | 3.0 |
| OM1 b | 56.3 | 25.3 | 13.1 | 1.1 | 3.7 |
| OM1 c | 60.3 | 20.6 | 14.2 | 1.0 | 3.7 |
| OM1 d | 58.1 | 23.7 | 14.1 | 1.0 | 3.7 |
| RR1 a | 56.8 | 23.6 | 13.5 | 3.2 | 1.9 |
| RR1 b | 56.2 | 24.1 | 14.3 | 2.5 | 2.0 |
| RR2 a | 60.0 | 23.6 | 9.6 | 1.3 | 4.7 |
| RR2 b | 60.2 | 24.6 | 8.1 | 2.3 | 3.8 |
| RR3 a | 61.8 | 23.9 | | | 2.5 |
| RR3 b | 60.6 | 25.0 | | | 2.8 |

Table 3. QXRD Summary: 95 % Confidence Limits for the Mean (Mass Percent).

| | Limits | | |
|------------------|---------------|-------------|--------------|
| | Lower | Mean | Upper |
| Alite | 56.50 | 56.75 | 57.00 |
| Belite | 20.91 | 21.04 | 21.17 |
| Aluminate | 3.41 | 3.46 | 3.50 |
| Ferrite | 14.40 | 14.61 | 14.81 |
| Periclase | 4.07 | 4.13 | 4.20 |

Graphical Analyses: Boxplots

The boxplot is a schematic graphical device for comparing the empirical distributions represented by batches of numbers [14]. For these data, the analytical method (QXRD, OM-1, RR1-n) separates the batches. This plot can be considered a visual one-way anova or t-test. The location of the distributions, their spread, and extremes are embedded in the graphical display. This allows meaningful comparison of distributional information through rapid assessment of the alignment or mis-alignment of median values and boxes, and differences in spread.

Important features of the boxplot are:

1. the width of the box is proportional to sample size,
2. the median value, used for its resistance to outliers, is identified by the X,
3. the interquartile range ("middle half") of the data are represented by the body of the box, and
4. the extremes (minimum and maximum) are represented by the ends of the straight lines projecting out of the box.

One important consideration for these data are that the QXRD box represents 36 numbers, the RM certificate data (OM) represents four numbers, and the round robin data (RR) represents two numbers each. The boxes for the RR groups, with only two observations, have the upper line of the box equal to one observation and data point, the other line equal to the other, and the X in the middle denoting the mean/median of the two observations.

Direct Phase Estimates by Microscopy and QXRD

Both microscopical and QXRD methods have been used to estimate phase abundance of clinker and are considered direct methods of analysis. Error in microscopy due to incorrect identification of the constituent phases is considered to exceed the error due to counting statistics [15] as fineness of the constituents may preclude their identification. For the finer-grained clinkers this may be especially problematic for the interstitial phases periclase, free lime, and the alkali sulfates.

X-ray powder diffraction analyses are not limited by crystal size and so are suitable for both clinker and cements. The accuracy of XRD, given careful experimental procedure, is about 2 % to 5 % absolute for alite and belite and 1 % to 2 % for aluminate and ferrite [15]. Limitations of the accuracy lie in the suitability of the reference standards (the structure models), and the ability

to identify and control correlations between variables. Generally, one should see good agreement between XRD and microscopy for the silicates and the total interstitial phases.

Alite (Figure 5) shows reasonable comparability among XRD, OM-1 and RR-1, with RR-2 and RR-3 being higher. OM-1 with its 4 points has significantly greater spread (IQ-range) than the more tightly grouped XRD numbers. For belite (Figure 6), the optical points diverge from the XRD yet demonstrate reasonable agreement along themselves, although OM-1 again displays large variance, with only the lowest point comparing favorably with XRD.

Aluminate values (Figure 7) do not demonstrate good agreement among XRD and optical data. Here OM-1 is a lowlier. This may result from the fine crystal size and resulting difficulty in seeing this phase. Ferrite estimates (Figure 8) exhibit reasonable agreement among XRD, OM-1, and RR-1, both in terms of level (mean/median) and spread. Periclase estimates (Figure 9) fall into two groupings with respect to the mean/median: XRD/OM/RR-2 versus RR-1/RR-3.

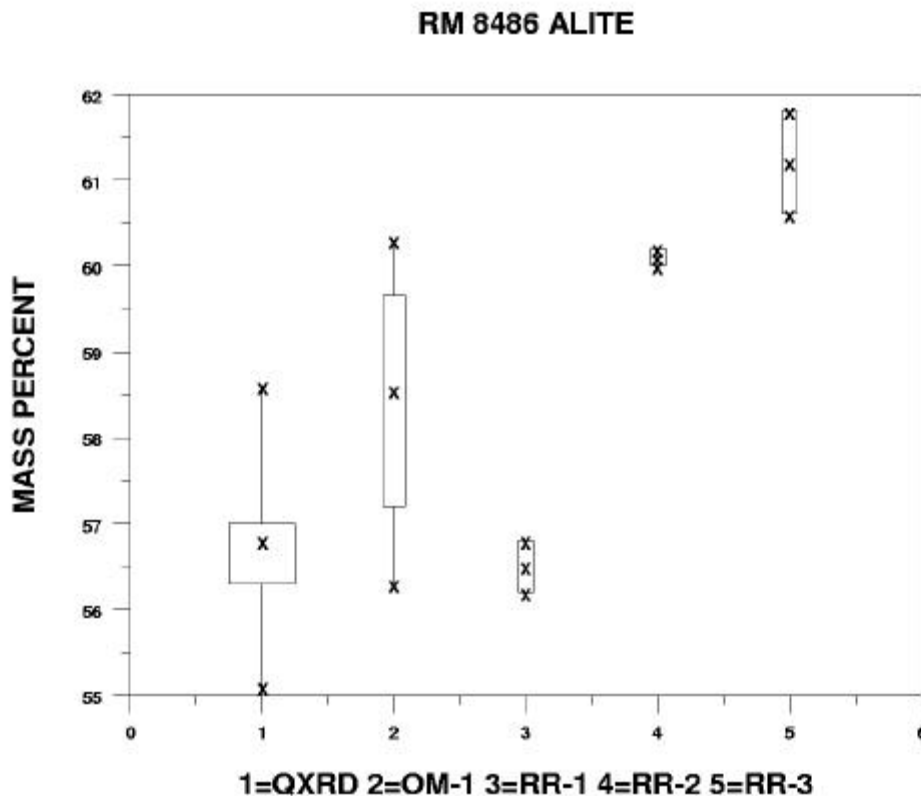


Figure 5. Boxplot representation of QXRD, optical microscopy (OM), and round robin (RR) data on phase abundance of alite.

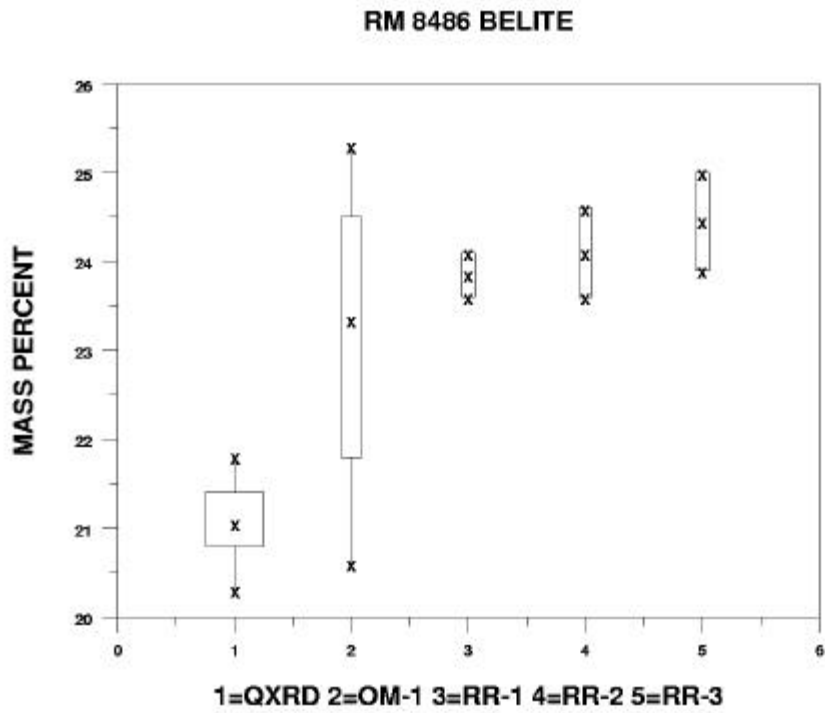


Figure 6. Boxplot on phase abundance of belite.

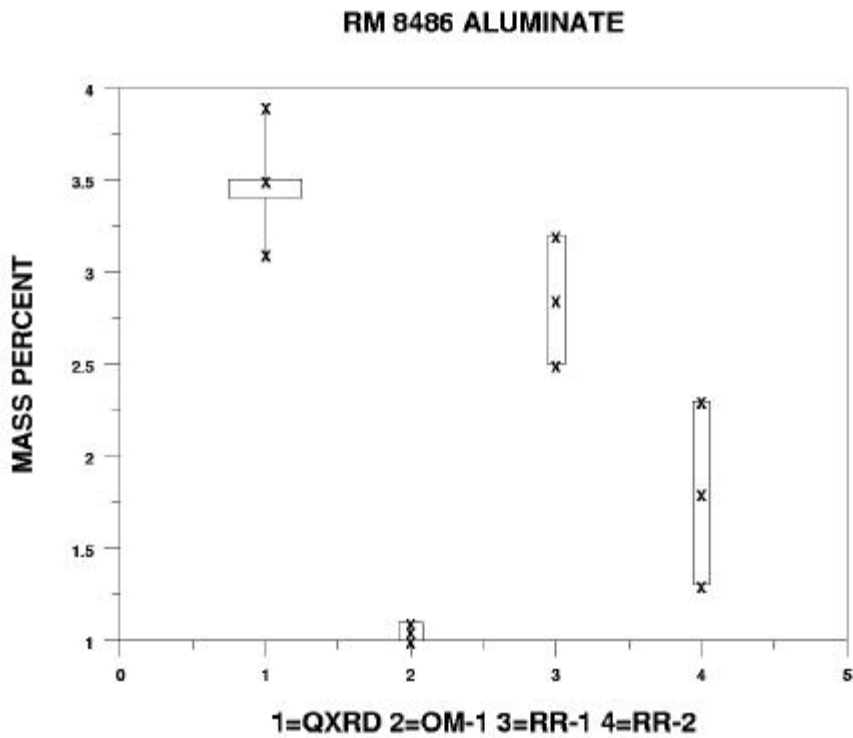


Figure 7. Boxplots on phase abundance of aluminate

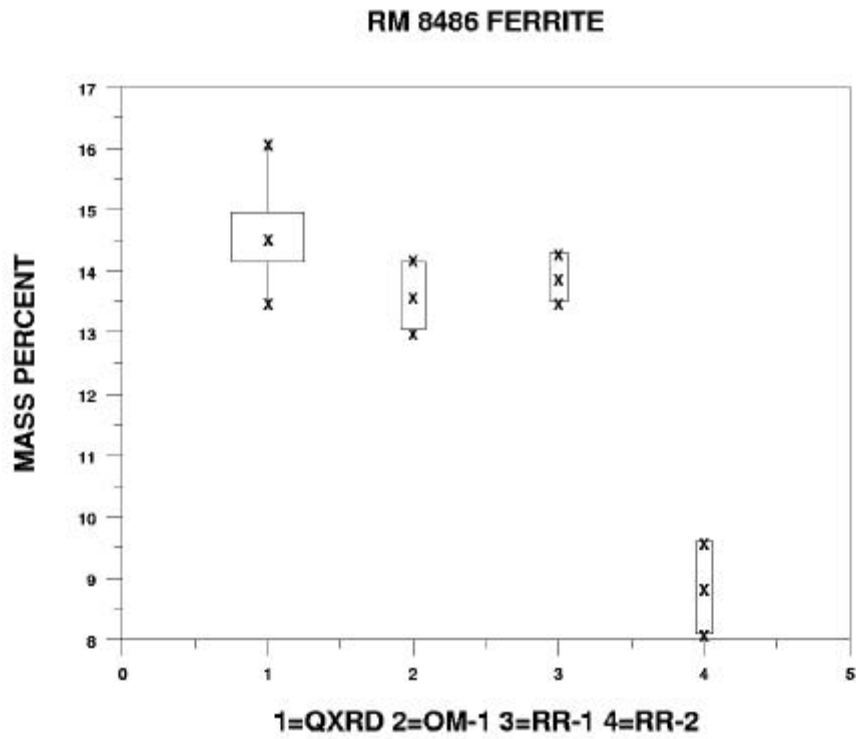


Figure 8. Boxplot on phase abundance of ferrite.

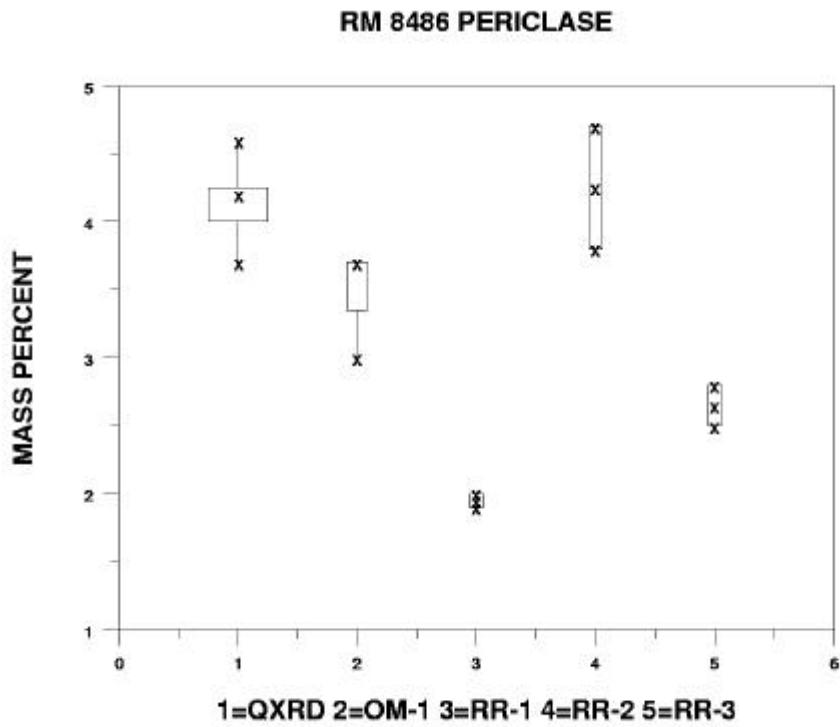


Figure 9. Boxplot on phase abundance of periclase.

Establishing Consensus Mean and Consensus Uncertainty for Phase Abundance

Measurements from different sources, different laboratories, different instruments, and different methods can exhibit significant between-method variability, as well as distinct within-method variances. Often a reference material is certified based on data from more than one measurement method. This situation occurs when no single method can provide the necessary level of accuracy and/or when there is no single method whose sources of uncertainty are well-understood and quantified. A common goal in the analysis of such data is to compute a best-consensus value and to attach a meaningful uncertainty to that value. The results of the combined XRD and optical microscopy data sets are presented in Table 4. Three methods of combining these data sets are presented and will be discussed below.

The Naive Method

A naive approach [16,17] is to regard the different method results for the same analyte as being repeated estimates of a single true mean, and to compute the consensus mean as the unweighted mean of the different group means, and the consensus uncertainty as:

$$t(n-1) \times \frac{(s)}{\sqrt{n}}$$

where n is the number of groups, the ordinary sample standard deviation s is computed on the mean values themselves, and " t " is the appropriate tabulated value of the Student t percent point function. A very high t value for the case $n=2$ ($t \approx 13$) typically precludes using this approach when only two groups are available. This method is useful in that it is simple, probably something that many practitioners would intuitively attempt to use, and will often give a consensus value identical or very close to other "naturally" weighted methods. The naive method also yields a less conservative uncertainty than those provided by other methods which take other sources of error into account.

The Levenson et al. Method

The point of departure for a new method of consensus mean/uncertainty estimation, proposed by Levenson et al. at NIST [18], is to note that the intent of using multiple methods is to realize systematic effects (biases) of individual methods as variation across the multiple methods results. However, if the number of methods is small--two to four--then the sample standard deviation of the method means will be a poor estimator of the uncertainty of the systematic effects. To overcome this, this method uses a Type B model [19] for the uncertainty of the systematic effects. In practice, a uniform distribution, bounded by the range of method results, has been found to be as effective as a Type B model. Other methods make explicit use of intermethod bias (or bias squared), computed as the difference between the largest and smallest group means or between the largest and grand average of the group means [20], as a proxy for between-method variance.

The Mandel-Paule-Vangel-Rukhin (MPVR) Method

Another approach to computing consensus estimates is to try to get an explicit estimate of the intermethod (intergroup) variance, and sum that with a pooled estimate of the within-method (within-group) variance, use the combination to weight the contributions from the different methods to form a consensus mean, and multiply by an appropriate expansion factor, e.g., 2, to get a nominal 95 % uncertainty interval. An estimation equation approach for the determination of the between-group variance developed by Mandel and Paule [21] has often been used at NIST, particularly in the certification of standard reference materials. Vangel-Rukhin [22] showed that the Mandel-Paule solution can be interpreted as a simplified version of maximum likelihood. While most useful when the number of contributing methods is large, we compute the MPVR estimates of the inter-method variances here and add them to a standard pooled estimates of the within method variances, take the square root to get an estimate of the overall standard errors, and multiply by an expansion factor of 2. This method has the virtue of explicitly quantifying within-group and between-group variation, and being rooted in a broadly applicable important general method of mathematical statistics, namely maximum likelihood. The drawback is that the estimation equation solution and formulations of its variance are asymptotically correct, so that MPVR estimates are better for data sets where many (e.g. >10) methods/groups are present.

Summary

Phase compositional data from X-ray powder diffraction were compared and combined with that obtained using optical microscopy for the NIST RM 8486 clinker. Rietveld refinement of the XRD data facilitated calculation of suitable reference standards for quantitative analyses. The optical data were collected using a point-counting procedure following ASTM C 1356.

Comparison of the phase composition data sets using boxplots provided a means of displaying and evaluating the data distributions, including their locations, spreads, and extremes. The data sets generally show reasonable agreement in the estimates of the individual phase abundance. The data do not agree as well in the estimate of aluminate content, with the optical data being significantly lower. This may be the result of the fine size of the aluminate crystals and the resulting difficulty in their microscope identification. The XRD data exhibit greater precision than that of the microscopy point counts. This may reflect the homogenization of the sample as a result of the fine grinding required for XRD analyses.

Measurements from different sources, laboratories, instruments, and from different methods can exhibit significant between-method variability, as well as distinct within-method variances. Certification of a Reference Material is often based upon more than one measurement method. X-ray powder diffraction and microscopy analyses are the intended use of these clinkers and so were used for determining the phase abundance. To establish best-consensus values and meaningful uncertainties, three methods of combining these data sets were used. The mean values of individual phase abundance do not vary from method to method, but the 95 % uncertainty interval values do depending upon the method. In selecting a single method to report consensus values, the MPVR would be favored as this method produces a weighted mean. The weighting scheme utilized does not necessarily skew the consensus value in the direction of the large number of XRD values and produces the most conservative uncertainty interval. The MPVR method also takes explicitly into account between- as well as within-method variance.

Table 4. Combined QXRD / Optical Analyses Mean and 95 % Uncertainty Interval.

| | ALITE | BELITE | FERRITE | ALUMINATE | PERICLASE |
|------------------------|--------------|---------------|----------------|------------------|------------------|
| Naive Method | 58.6 | 23.3 | 14.1* | 2.3 | 3.3 |
| 2-s | 2.6 | 1.7 | 1.0 | 1.7 | 1.2 |
| Levenson et al. | 58.6 | 23.3 | 14.1 | 2.3 | 3.3 |
| 2-s | 2.8 | 2.2 | 1.1 | 1.5 | 1.4 |
| MPVR | 58.6 | 23.3 | 14.1* | 2.3 | 3.3 |
| 2-s | 4.0 | 2.8 | 1.4 | 2.1 | 1.9 |

* ferrite mean and 2- σ values are based upon 2-source (XRD, OM-1) data alone.

Acknowledgements:

The authors gratefully acknowledge the comments and suggestions of the reviewers, Clarissa Ferraris, Edward Garboczi, and Louis Jany. This work was supported by the Partnership on High Performance Concrete Technology and the Standard Reference Materials Program at the National Institute of Standards and Technology.

References:

1. Report of Investigation, Reference Materials 8486, 8487, 8488, National Institute of Standards and Technology.
2. ASTM C 1356M - 96 Standard Test Method for Quantitative Determination of Phases in Portland Cement Clinker by Microscopical Point-Count Procedure. In Annual Book of ASTM Standards Vol. 4.01 American Society for Testing and Materials, West Conshohocken, PA1999
3. D.H. Campbell, Microscopical Examination and Interpretation of Portland Cement and Clinker, 2nd ed., The Portland Cement Association Research and Development Serial No. 1754, 1999, 202 pp.
4. ASTM C 1365 - 98 Standard Test Method for Determination of the Proportion of Phases in Portland Cement and Portland Cement Clinker Using X-Ray Powder Diffraction Analysis. In Annual Book of ASTM standards Vol. 4.01 American Society for Testing and Materials, West Conshohocken, PA1999
5. R.A. Young, ed., The Rietveld Method, International Union of Crystallography Monographs on Crystallography 5, Oxford University Press
6. A.C. Larson and R.B. VonDreele, "GSAS General Structure Analysis System," Operational Manual, Los Alamos National Laboratory LAUR 86-748

7. F. Nishi, Y. Takouchi and I. Maki, "Tricalcium silicate $\text{Ca}_3\text{O}[\text{SiO}_4]$: The monoclinic superstructure," *Zeitschrift für Kristallographie* 172, 297-314 (1985)
8. P. Mondal and J.W. Jeffery, "The crystal structure of tricalcium aluminate, $\text{Ca}_3\text{Al}_2\text{O}_6$," *Acta Cryst.*, (1975). **B31** 689.
9. K.H. Jost, B. Ziemer, and R. Seydel, "Redetermination of the structure of β -dicalcium silicate," *Acta Cryst.* (1977) **B33**, 1696-1700.
10. A.A. Colville and S. Geller, "The crystal structure of Brownmillerite, $\text{Ca}_2\text{FeAlO}_5$," *Acta Cryst.* (1971) **B27**, 2311.
11. Y. Takouchi, F. Nishi, and I. Maki, "Crystal-chemical characterization of the 3 CaO \cdot Al_2O_3 - Na_2O solid solution series," *Zeitschrift für Kristallographie* 152, 259-307 (1980).
12. W.A. Klemm and J. Skalny, "Selective Dissolution of Clinker Minerals and Its Applications, Martin Marietta Technical Report 77-32, 1977, 26 pp.
13. J.C. Taylor and C.E. Matulis, "Absorption Contrast Effects in the Quantitative XRD Analysis of Powders by Full Multi-phase Profile Refinement," *J. Appl. Cryst.* (1991) 24, 14-17.
14. H.F.W. Taylor, Cement Chemistry, 2nd edition, Thomas Telford, London, 1997, 459 pp.
15. Neter, J. Kutner, M.H. Nachtsheim, C.J., Wasserman, W., APPLIED LINEAR STATISTICAL MODELS Irwin/McGraw-Hill Chicago 1996
16. Taylor, B.N. and Kuyatt, Chris E. "Guidelines for Evaluating and Expressing the Uncertainty of NIST Measurement Results," NIST Technical Note 1297 USDOC 1994.
17. M.S. Levenson D.L. Banks K.R. Eberhardt, L.M. Gill, W.F. Guthrie, H.K. Liu, M.G. Vangel, J.H. Yen, and N.F. Zhang, "An ISO GUM Approach to Combining Results from Multiple Methods," to appear NIST JOUR RESEARCH 2000
18. Guide to the Expression of Uncertainty in Measurement ISO Switzerland 1st ed. 1993.
19. S.B. Schiller and K.R. Eberhardt, "Combining data from independent chemical analysis methods" *Spectrochimica Acta* vol. 46B, no. 12, 1991 pp. 1607-1613.
20. A. Heckert and J. J. Filliben, Dataplot Reference Manual , <http://www.itl.nist.gov/div898/software/dataplot/>
21. Mandel, J., EVALUATION AND CONTROL OF MEASUREMENTS Marcel Dekker, New York, 1991 sections 4.4-4.5
22. Rukhin, A.L. Vangel, M.G., "Estimation of a Common Mean and Weighted Means Statistics," *JOURNAL OF THE AMERICAN STATISTICAL ASSOCN.* March 1998 vol. 93 no. 441 pp. 303-308